Journal of Nuclear Medicine, published on May 25, 2023 as doi:10.2967/jnumed.122.265252

Delayed Imaging Improves Lesion Detectability in [^{99m}Tc]Tc-PSMA-I&S SPECT/CT in Recurrent Prostate Cancer

Christoph Berliner*[1,2], Lisa Steinhelfer*[3], Maythinee Chantadisai[3], Markus Kroenke[3], Daniel Koehler[1], Randi Pose[4], Peter Bannas[1], Sophie Knipper[4], Matthias Eiber†[4], and Tobias Maurer†[4,5]

[1]*Department of Diagnostic and Interventional Radiology and Nuclear Medicine, Universitätsklinikum Hamburg–Eppendorf, Hamburg, Germany;* [2]*Department of Nuclear Medicine, Universitätsklinikum Essen, Essen, Germany;* [3]*Department of Nuclear Medicine, Klinikum Rechts der Isar, Technische Universität München, München, Germany;* [4]*Martini-Klinik Prostate Cancer Center, University Hospital Hamburg–Eppendorf, Hamburg, Germany; and* [5]*Department of Urology, University Hospital Hamburg–Eppendorf, Hamburg, Germany*

Our objective was to compare the ability to detect histopathologically confirmed lymph node metastases by early and delayed [^{99m}Tc]Tc-PSMA-I&S SPECT/CT in early biochemically recurrent prostate cancer. **Methods:** We retrospectively analyzed 222 patients selected for radioguided surgery using [^{99m}Tc]Tc-PSMA-I&S SPECT/CT at different time points after injection (≤4 h and >15 h). In total, 386 prostate-specific membrane antigen (PSMA) PET predetermined lesions were analyzed on SPECT/CT using a 4-point scale, and the results were compared between early and late imaging groups, with uni- and multivariate analyses performed including prostate-specific antigen, injected [^{99m}Tc]Tc-PSMA-I&S activity, Gleason grade group, initial TNM stage, and, stratified by size, PSMA PET/CT–positive lymph nodes. PSMA PET/CT findings served as the standard of reference. **Results:** [^{99m}Tc]Tc-PSMA-I&S SPECT/CT had a significantly higher positivity rate for detecting lesions in the late than the early imaging group (79%, $n = 140/178$, vs. 27%, $n = 12/44$ [$P < 0.05$] on a patient basis; 60%, $n = 195/324$, vs. 21%, $n = 13/62$ [$P < 0.05$] on a lesion basis). Similar positivity rates were found when lesions were stratified by size. Multivariate analysis found that SUV_{max} on PSMA PET/CT and the uptake time of [^{99m}Tc]Tc-PSMA-I&S were independent predictors for lesion detectability on SPECT/CT. **Conclusion:** Late imaging (>15 h after injection) should be preferred when [^{99m}Tc]Tc-PSMA-I&S SPECT/CT is used for lesion detection in early biochemical recurrence of prostate cancer. However, the performance of PSMA SPECT/CT is clearly inferior to that of PSMA PET/CT.

Key Words: prostate carcinoma; scintigraphy; radioguided; salvage surgery; biochemical recurrence; PET

J Nucl Med 2023; 00:1–7
DOI: 10.2967/jnumed.122.265252

Prostate cancer is one of the most diagnosed cancers and the fourth leading cause of cancer-related death in men worldwide (*1*). Definitive surgery or radiotherapy is currently the curative therapy of choice (*2*). Success rates are measured in biochemical recurrence (BCR)–free survival. However, a portion of patients experiences recurrence after initial surgical treatment (*3–6*) as determined by a rising blood level of prostate-specific antigen (PSA). A confirmed increase in PSA greater than 0.2 ng/mL during follow-up after radical prostatectomy (RP) defines BCR (*2*). For further therapy and management, it is crucial to recognize and differentiate between local, regional, and systemic prostate recurrence (*7,8*).

In the last decade, hybrid imaging with prostate-specific membrane antigen (PSMA) ligands has emerged as the most accurate imaging modality to detect lesions in early BCR (*9–12*). Several radiopharmaceuticals targeting PSMA are available and in clinical use (*13–15*). PSMA ligands labeled with γ-emitters allow new therapeutic options in BCR, such as PSMA radioguided surgery (RGS) (*16,17*). Their signal can also be used for SPECT imaging (*18*). Compared with PET/CT scanners, SPECT/CT scanners are less costly and more accessible in most parts of the world. Therefore, the diagnostic performance of ^{99m}Tc-labeled PSMA ligands for SPECT imaging and its comparison to PET imaging is of the utmost interest, but so far, data are sparse, especially in early BCR (*19*).

PSMA-targeting radiopharmaceuticals are internalized, and lesion-to-background contrast improves over time (*20*). These dynamics may be especially relevant for PSMA ligands labeled by nuclides with longer half-lives. Despite established use in RGS, the optimal time interval for [^{99m}Tc]Tc-PSMA-I&S injection and SPECT imaging is not known to date.

The aim of this retrospective analysis was to compare early (≤4 h after injection) and late (≥15 h after injection) [^{99m}Tc]Tc-PSMA-I&S SPECT/CT imaging for the identification of pelvic lymph node metastases in early BCR.

MATERIALS AND METHODS

Study Population

We retrospectively reviewed the databases at 2 centers for all patients who underwent RGS using [^{99m}Tc]Tc-PSMA-I&S between September 2015 and April 2020.

Patients were included if they had BCR after RP and PSMA PET/CT–positive pelvic or retroperitoneal soft-tissue metastases, had undergone [^{99m}Tc]Tc-PSMA-I&S SPECT/CT before RGS, and had all imaging data available in a digital format. The obtained PSMA PET/CT scan served as the diagnostic gold standard, and only PET-positive

Received Dec. 6, 2022; revision accepted Mar. 7, 2023.
For correspondence or reprints, contact Christoph Berliner (christoph.berliner@uk-essen.de).
*Contributed equally to this work.
†Contributed equally to this work.
Published online May. 25, 2023.

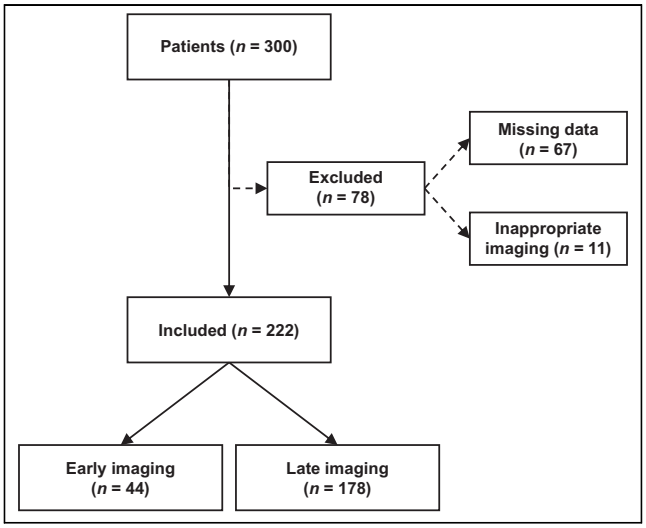

FIGURE 1. Flowchart of included patients. Total of 222 of 300 patients in our institutional databases met inclusion criteria for analysis. We excluded 78 patients (incomplete availability of imaging data [$n = 67$], staging images provided as PSMA PET/MRI [$n = 10$], or staging images provided as choline PET/CT [$n = 1$]).

patients were included in the analysis. All lesions were histopathologically confirmed after salvage surgery.

Patients were excluded from analysis if data were missing (unavailable image data) or if inappropriate imaging had been performed (an imaging modality other than PSMA PET/CT or a tracer for SPECT/CT and PSMA RGS other than [^{99m}Tc]Tc-PSMA-I&S).

Finally, 222 patients could be included in the retrospective analysis (Fig. 1). The initial patient characteristics and findings before RGS are shown in Table 1 and Supplemental Table 1 (supplemental materials are available at http://jnm.snmjournals.org). The local ethics committees (PV7316 and 226/18S) approved this retrospective study, and the requirement to obtain informed consent was waived.

[^{99m}Tc]Tc-PSMA-I&S SPECT/CT Imaging and Interpretation

The application of [^{99m}Tc]Tc-PSMA-I&S was part of the RGS (*21*). [^{99m}Tc]Tc-PSMA-I&S was prepared as described previously (*17*). The administration of [^{99m}Tc]Tc-PSMA-I&S complied with the German Medicinal Products Act, Arzneimittelgesetz §13 2b, and the responsible regulatory bodies. All patients underwent whole-body planar imaging and pelvic [^{99m}Tc]Tc-PSMA-I&S-SPECT/CT no more than 4 h after injection or at least 15 h after injection (Supplemental Table 2).

PSMA PET/CT and [^{99m}Tc]Tc-PSMA-I&S SPECT/CT images were reanalyzed independently by 2 physicians experienced in nuclear medicine and radiology. Axial, sagittal, and coronal SPECT, PET, and

TABLE 1
Characteristics of 222 Patients Treated with RGS Between 2014 and 2020 at 2 Centers*

Parameter	Early SPECT (≤4 h after injection; $n = 44$)	Late SPECT (≥15 h after injection; $n = 178$)	*P*
Year of initial RP	2010 (2005–2013)	2014 (2010–2016)	<0.001
PSA at RP (ng/mL)	10 (6–16)	9 (6–15)	0.8
Lymph node yield at RP	13 (8–20)	13 (8–20)	0.6
Positive lymph nodes at RP			0.6
0	32 (73)	115 (65)	
1	3 (6.8)	19 (11)	
2	3 (6.8)	9 (5.1)	
≥3	2 (4.5)	5 (2.8)	
Unknown	4 (9.1)	30 (17)	
Surgical margin status			0.05
R0	29 (66)	130 (73)	
R1	9 (20)	41 (23)	
RX/NA	6 (14)	7 (3.9)	
RT after RP			0.1
No RT	15 (34)	59 (33)	
RT after RP	28 (64)	119 (67)	
NA	1 (2.3)	0 (0)	
Time from RP to SPECT (mo)	70 (22–128)	46 (22–88)	0.2
Age at PSMA RGS (y)	72 (65–75)	66 (61–70)	<0.001
PSA before SPECT (ng/mL)	1.4 (0.7–3.0)	1.0 (0.5–2.0)	0.09

*Patients received [^{99m}Tc]Tc-PSMA-I&S SPECT/CT before surgery and presented with BCR after RP with histopathology-confirmed positive lesions at PSMA PET/CT.

NA = not assigned; RT = radiotherapy.

Qualitative data are number and percentage; continuous data are median and IQR.

TABLE 2
PSMA PET/CT and SPECT/CT Imaging Characteristics of 222 Patients with BCR After RP Treated with RGS Between 2014 and 2020 at 2 Centers Within Early and Late [^{99m}Tc]Tc-PSMA-I&S SPECT/CT Groups

Parameter	Early SPECT (≤4 h after injection; n = 44)	Late SPECT (≥15 h after injection; n = 178)	P
Lesions on PSMA PET			0.7
1	30 (68%)	94 (53%)	
2	11 (25%)	53 (30%)	
3	2 (4.5%)	16 (9.0%)	
4	1 (2.3%)	7 (3.9%)	
≥5	0 (0%)	8 (4.5%)	
Maximum lesion size on PET/CT (mm)	8 (7–12)	9 (6–12)	0.7
Maximum lesion SUV on PET	9 (6–17)	8 (5–16)	0.1
Ratio of maximum lesion SUV to background on PET	12 (7–22)	8 (5–16)	0.02
miTNM-Tr	0 (0%)	28 (16%)	0.01
miTNM-N1	34 (77%)	112 (63%)	0.1
miTNM-N2	10 (23%)	53 (30%)	0.5
miTNM-M1a	0 (0%)	15 (8.4%)	0.1
[^{99m}Tc]Tc-PSMA-I&S activity (MBq)	550 (416–702)	752 (695–786)	<0.001
Corrected [^{99m}Tc]Tc-PSMA-I&S activity at time of SPECT (MBq)	488 (370–632)	99 (91–108)	<0.001
Interval between [^{99m}Tc]-Tc-PSMA-I&S tracer injection and SPECT imaging (h)	1.0 (1.0–2.0)	18.0 (17.0–18.0)	<0.001
Lesions on SPECT			<0.001
0	33 (75%)	45 (25%)	
1	9 (20%)	90 (51%)	
2	1 (2%)	27 (15%)	
3	1 (2%)	13 (7%)	
4	0 (0%)	2 (1%)	
≥5	0 (0%)	1 (1%)	
Maximum lesion size on SPECT/CT (mm)	11.5 (7.8–17.1)	9.0 (7.0–13.0)	0.07

Qualitative data are number and percentage; continuous data are median and IQR.

CT images as well as fused images were analyzed using OsiriX MD (Pixmeo) (*22*).

For PET data analysis, a 40% isocontour volume of interest was drawn around suggestive areas, with added volumes of interest in the background (blood pool, gluteal muscle). SUV_{max} and SUV_{mean} were recorded. SPECT lesion detectability was assessed qualitatively using a 4-point scale (Supplemental Table 3).

To assess potential differences between early (≤4 h after injection) and late (≥15 h after injection) [^{99m}Tc]Tc-PSMA-I&S SPECT/CT imaging, the patient cohort was divided into 2 groups. Patients in the early imaging group underwent [^{99m}Tc]Tc-PSMA-I&S-I&S 1–4 h after injection (median, 1 h; interquartile range [IQR], 1–2 h), and patients in the late imaging group underwent imaging at 15–20 h after injection (median, 18 h; IQR, 17–18 h). The mean injected activities were 560 ± 201 MBq (IQR, 417–702 MBq) and 733 ± 90 MBq (IQR, 695–786 MBq) in the early and late imaging groups, respectively (Table 2).

Statistical Analysis

Descriptive statistics included frequencies and proportions for categoric variables and means, medians, and IQR for continuous variables. Test power was calculated using a t-statistical power calculator with a medium effect size of 0.5 and a significance level of 0.05. Differences in medians and proportions between early and late imaging were evaluated using Kruskal–Wallis, Mann–Whitney U, Fisher exact, and χ^2 tests (*23,24*).

Univariable and multivariable logistic regression models tested the relationship between visibility of lesions on SPECT before PSMA RGS and the following clinical variables: Gleason grade group at RP (I-II vs. III-V), pT stage at RP (pT2 vs. pT3a/b), pN stage at RP (pN0/NX vs. pN1), margin status at RP (R0 vs. R1), radiation therapy after RP before PSMA RGS (yes vs. no), time between initial RP and SPECT, age at SPECT, number of PSMA PET–positive lesions, maximal size of PSMA PET–positive lesions on PET/CT, SUV_{max} of PSMA PET–positive lesions, [^{99m}Tc]Tc-PSMA-I&S activity, and time interval between [^{99m}Tc]Tc-PSMA-I&S tracer injection and SPECT imaging. Predictors were included in the multivariable models if significantly associated with the outcome in the univariable analysis.

For all statistical analyses, the R software environment for statistical computing and graphics (version 3.4.3) was used. All tests were 2-sided, with the level of significance set at a P value of less than 0.05.

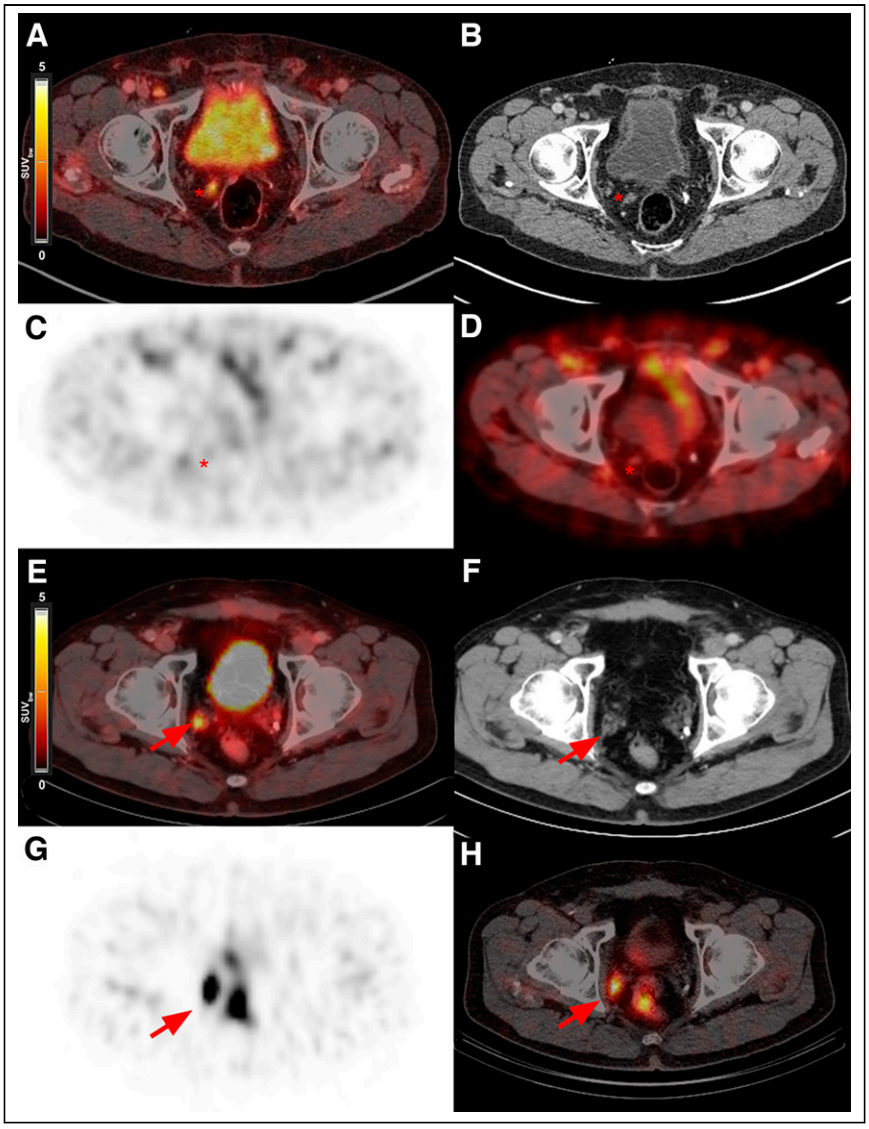

FIGURE 2. Examples of early (A–D) and late (E–H) [^{99m}Tc]Tc-PSMA-I&S SPECT/CT imaging. (A–D) In 74-y-old patient who had RP in 2004 and BCR in 2016 (PSA, 0.66 ng/mL), PSMA PET (A and B) shows local recurrence in right prostate fossa with intense PSMA expression (SUV_{max}, 12.7 [asterisk]); 4 h after [^{99m}Tc]Tc-PSMA I&S injection, SPECT/CT (C and D) morphologically identifies known local recurrent cancer (asterisk) but uptake is not above background, with overall score of 2. (E–H) In 66-y-old patient who had RP in 2012 and BCR in 2018 (PSA, 0.59 ng/mL), PSMA PET (E and F) shows right internal iliac lymph node metastasis with intense PSMA expression (SUV_{max}, 5.0 [arrow]); 18 h after [^{99m}Tc]Tc-PSMA-I&S injection, SPECT/CT (G and H) confirms metastasis with significant uptake above background (score 4, arrow).

RESULTS

Patient-Based Analysis

Overall, 65% (144/222) of all patients had at least 1 lesion scored as visible on SPECT (Table 2). On a patient basis, at least 1 lesion was present in 25% (11/44) and 75% (133/178) of patients in the early versus late imaging groups. Representative patient examples are shown in Figure 2. There was a strong power (0.84) in the t-statistical test. No difference between groups was found in number of lesions, SUV_{max} of the hottest lesion, or lesion size. However, the early imaging group had a higher lesion-to-background SUV_{max} ratio on PET (Table 2).

Lesion-Based Analysis

In total, 386 lesions could be identified in 222 patients on PET/CT imaging. Of these, 208 (54%) were scored as detectable on SPECT/CT. Late SPECT/CT imaging revealed a significantly higher percentage of lesions than was seen on early SPECT/CT (60%, $n = 195/324$, vs. 21%, $n = 13/62$ [$P < 0.05$]). Similar results were present when lesions were stratified by size, at 0%, 10%, 11%, and 62% vs. 52%, 50%, 66%, and 78% for lesions sized 1–3, 4–7, 8–10, and greater than 10 mm on early versus late imaging, respectively (Fig. 3).

The results were stratified into different PSA subgroups. Only in patients with a PSA of less than 0.2 ng/mL was no significant difference in lesion detectability seen on late versus early SPECT/CT imaging (56%, 9/16, vs. 100%, 2/2 [$P = 0.49$]). Lesion detectability was higher on late than early imaging in patients with a PSA of 0.2 to less than 0.5 ng/mL (41%, 25/61, vs. 0%, 0/0 [$P < 0.001$]), a PSA of 0.5 to less than 1 ng/mL (57%, 38/67, vs. 0%, 0/9 [$P < 0.002$]), a PSA of 1 to less than 2 ng/mL (60%, 52/86, vs. 0%, 0/11 [$P < 0.001$]), and PSA of more than 2 ng/mL (76%, 71/94, vs. 34%, 11/32 [$P < 0.001$]).

PET SUV_{max} and Interval Between Tracer Injection and SPECT Imaging as Independent Factors Predicting SPECT Detectability

Univariate regression found PSA, number of lesions on prior PSMA PET, maximum lesion size on PSMA PET/CT, SUV_{max} of lesions on prior PSMA PET, injected tracer activity ([^{99m}Tc]Tc-PSMA-I&S), and interval between tracer injection and SPECT imaging significant for lesion detectability (all $P < 0.05$, Table 3).

Multivariate regression showed only SUV_{max} of prior PET/CT lesions and time interval between tracer injection and SPECT as independent SPECT detectability factors ($P < 0.05$, respectively). PSA at SPECT imaging ($P = 0.09$), number of PET/CT-detected lesions ($P = 0.07$), maximum size of lesions ($P = 0.2$), and activity of injected [^{99m}Tc]Tc-PSMA-I&S ($P = 0.6$) failed to show a significant correlation in our patient cohort.

DISCUSSION

Our study compared early (1–4 h) versus late (15–20 h) [^{99m}Tc]Tc-PSMA-I&S SPECT/CT imaging for detecting tumors in prostate cancer patients. Late imaging was found to be more advantageous, especially for tumors smaller than 10 mm, and was an independent predictor for detecting lesions. Lesion SUV_{max} on PSMA PET and detectability on late SPECT/CT were the main factors for depicting PSMA PET–avid lesions, with PSA, number of

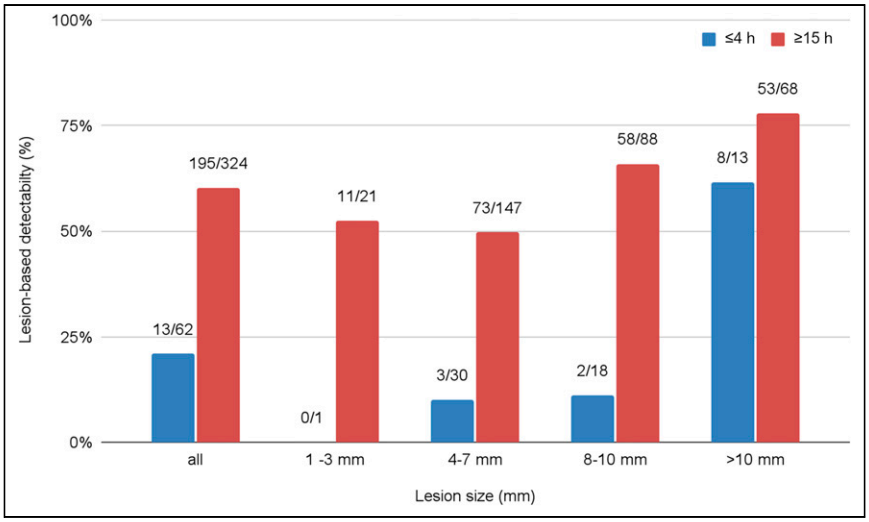

FIGURE 3. Overall and size-dependent lesion-based detectability by early (≤4 h) vs. late (≥15 h) [^{99m}Tc]Tc-PSMA-I&S SPECT/CT imaging.

lesions, and size not having a significant impact. Overall, the results indicate a preference for late-time-point imaging.

PSMA ligands attached to the binding sites of PSMA are usually internalized into the cell and degraded (*25*), entrapping the PSMA ligand. This active internalization process provides an advantage for small diagnostic molecules, as they are pooled over time in cells with high PSMA expression, such as most prostate cancer cells. On the other hand, the physical decay of radioisotopes lowers the absolute measurable activity within PSMA-positive cells over time. For ^{68}Ga-based PSMA PET tracers, reports indicate that a late time point at 3 h shows slight advantages for lesion detection (*26*), although for practical reasons the clinically recommended time window is 1 h after injection (*27*). For most ^{18}F-based PSMA

TABLE 3
Uni- and Multivariable Logistic Regression Models Regarding Visibility of Lesions in [^{99m}Tc]Tc-PSMA-I&S SPECT/CT Imaging

	Univariable				Multivariable			
Variable	OR	CI, 2.5%	CI, 97.5%	*P*	OR	CI, 2.5%	CI, 97.5%	*P*
Gleason grade group at RP								
I–II	Ref.							
III–V	0.34	0.74	2.42	0.3				
pT stage at RP								
pT2	Ref.							
pT3a/b	0.65	0.34	1.21	0.2				
pN stage at RP								
pN0/X	Ref.							
pN1	0.53	0.27	1.05	0.07				
Margin status at RP								
R0	Ref.							
R1	1.0	0.51	2.06	0.9				
RT after RP								
No	Ref.							
Yes	0.82	0.43	1.49	0.5				
Time from RP to SPECT (continuous)	0.99	0.99	1.0	0.8				
Age at SPECT (continuous)	0.99	0.95	1.03	0.6				
PSA at SPECT (continuous)	1.21	1.03	1.47	0.03	1.25	0.99	1.66	0.09
Lesions on PET (continuous)	2.03	1.38	3.21	0.001	1.57	1.02	2.67	0.07
Maximum lesion size on PET (continuous)	1.13	1.05	1.22	0.002	1.06	0.97	1.17	0.2
Maximum lesion SUV on PET (continuous)	1.10	1.05	1.16	<0.001	1.15	1.07	1.27	<0.001
Activity of injected [^{99m}Tc]Tc-PSMA-I&S (continuous)	1.00	1.00	1.00	<0.001	0.99	0.99	1.0	0.6
Interval between injection and SPECT (continuous)	1.16	1.11	1.22	<0.001	1.27	1.17	1.40	<0.001

OR = odds ratio; RT = radiotherapy.

tracers, an uptake time of between 90 and 120 min is typically recommended (*28*). For ^{99m}Tc-based PSMA tracers, data in the literature are sparse and only a few publications indicate an average time range of 3–5 h (*19,29,30*). However, initial studies with PSMA RGS have shown an advantage of imaging after 18–24 h after injection (*17,31*).

In our retrospective analysis, significantly more pelvic lymph node metastases were detected on late than early SPECT/CT imaging, both on a patient basis and on a lesion basis. In comparison, Werner et al. showed in 2 cases that uptake remained high in lymph node metastases on planar scintigraphy at 20 h after injection (*19*). Of note, even on late SPECT/CT imaging, the total number of lesions was substantially less than on the PSMA PET/CT serving as the standard of reference. This finding is congruent with a report by Albalooshi et al. of a high and comparable sensitivity in bone metastasis with a PSA cutoff of more than 2.1 ng/mL but an inferior sensitivity with lower PSA levels (*29*). [^{99m}Tc]Tc-PSMA-I&S is currently only seldom used for staging purposes. Our study sheds new light on potential application scenarios for imaging with [^{99m}Tc]Tc-PSMA-I&S. We can envision that the use of late imaging [^{99m}Tc]Tc-PSMA-I&S SPECT/CT is adequate when the focus is more on the extent of disease before or during systemic treatment than on depiction of all lesions for potential metastasis-directed treatments. Here, patients with advanced disease could represent a cohort suitable for [^{99m}Tc]Tc-PSMA-I&S SPECT, for example, in therapy monitoring of metastatic castration-sensitive as well as castration-resistant patients after chemotherapy or [^{177}Lu]-Lu-PSMA radioligand therapy. Werner et al. have already delivered their first experiences (*19*). The advantage of SPECT/CT imaging lies in its lower costs and broader availability.

The advantages of late imaging were most apparent in small lesions and low PSA levels. The advantages are related to a significantly higher tumor-to-background ratio at late imaging, as a lower count rate in lesions is overcompensated by a diminishing activity in background tissue at the time of imaging. The overall decay of background activity was shown nicely by Urbán et al. in their dosimetry study (*32*). Nevertheless, the tumor-to-background ratio is still clearly inferior to that of PET imaging. These results are not unexpected given the physiologic characteristics of PSMA and the technical and physical limitations of SPECT compared with PET. To exclude test influences due to group invariance, we proved that there was no significant difference between patient characteristics, lesion size, and SUV_{max} of lesions on PET.

Our analysis had several limitations. First, the focus was on a specific cohort of patients with biochemically recurrent prostate cancer and PSMA PET–positive, histologically proven lymph node metastases within the pelvic region. This is a narrow patient population, and our results therefore might not be transferable to other patient populations without further investigation. Second, the size of the early and late imaging groups substantially differed, with 44 patients in the early group and 178 patients in the late group. Although we performed a t-statistical power analysis and Kruskal–Wallis tests, the results of these tests do not cover all eventualities and a possible bias remains. Third, the activity levels injected into the patients in both groups differed significantly, with a lower remaining physical activity in the late imaging group. Nevertheless, lesion detectability was still superior in this group, making the observation even more robust. Fourth, the exact kinetics of [^{99m}Tc]Tc-PSMA-I&S over time are still not known, and we had to use an approximation based on physical decay, which neglects potential trapping or detrapping of the agent over time. Finally, the retrospective nature of this study cannot exclude other influencing factors and invariances besides the tested factors.

CONCLUSION

For lesion detection in early BCR of prostate cancer, late imaging (≥15 h after injection) is preferred using [^{99m}Tc]Tc-PSMA-I&S SPECT/CT. It requires a 2-d protocol and is still clearly inferior to PET/CT imaging for primary staging, but it significantly improves image quality and the detectability of pelvic lesions.

DISCLOSURE

Christoph Berliner reports fees from ABX (consultant) and Janssen (speakers' bureau). Tobias Maurer reports fees from ABX, Advanced Accelerator Applications, Novartis, Telix, ROTOP Pharma, GEMoAb, Astellas, and Blue Earth Diagnostics (consultant) and from Bayer, Sanofi-Aventis, Astellas, and Phillips (speakers' bureau). Matthias Eiber holds parts of the patent for rhPSMA and received payments from third party funding from Blue Earth Diagnostics as well as consulting fees from Blue Earth Diagnostics, Novartis, Telix, Bayer, Point Biopharma, and Janssen. No other potential conflict of interest relevant to this article was reported.

KEY POINTS

QUESTION: Does delayed imaging improve the detectability of soft-tissue lesions on [^{99m}Tc]Tc-PSMA-I&S SPECT/CT?

PERTINENT FINDINGS: Late [^{99m}Tc]Tc-PSMA-I&S SPECT/CT imaging requires a 2-d protocol but significantly improves image quality and the detectability of soft-tissue lesions.

IMPLICATIONS FOR PATIENT CARE: [^{99m}Tc]Tc-PSMA-I&S SPECT/CT is still clearly inferior to PET/CT imaging for primary staging but could play a role in certain clinical scenarios focusing more on determining the extent of disease (e.g., for monitoring of systemic treatment) than on visualizing every lesion before metastasis-directed therapy.

REFERENCES

1. Sung H, Ferlay J, Siegel RL, et al. Global cancer statistics 2020: GLOBOCAN estimates of incidence and mortality worldwide for 36 cancers in 185 countries. *CA Cancer J Clin.* 2021;71:209–249.
2. Prostate cancer. European Association of Urology website. https://uroweb.org/guideline/prostate-cancer/. Accessed May 2, 2023.
3. Boehm K, Schiffmann J, Tian Z, et al. Five-year biochemical recurrence-free and overall survival following high-dose-rate brachytherapy with additional external beam or radical prostatectomy in patients with clinically localized prostate cancer. *Urol Oncol.* 2016;34:119.e11–119.e18.
4. Brockman JA, Alanee S, Vickers AJ, et al. Nomogram predicting prostate cancer-specific mortality for men with biochemical recurrence after radical prostatectomy. *Eur Urol.* 2015;67:1160–1167.
5. Lee BH, Kibel AS, Ciezki JP, et al. Are biochemical recurrence outcomes similar after radical prostatectomy and radiation therapy? Analysis of prostate cancer-specific mortality by nomogram-predicted risks of biochemical recurrence. *Eur Urol.* 2015;67:204–209.
6. Tyson MD, Penson DF, Resnick MJ. The comparative oncologic effectiveness of available management strategies for clinically localized prostate cancer. *Urol Oncol.* 2017;35:51–58.
7. Bott SRJ. Management of recurrent disease after radical prostatectomy. *Prostate Cancer Prostatic Dis.* 2004;7:211–216.
8. Valle LF, Lehrer EJ, Markovic D, et al. A systematic review and meta-analysis of local salvage therapies after radiotherapy for prostate cancer (MASTER). *Eur Urol.* 2021;80:280–292.
9. Anttinen M, Ettala O, Malaspina S, et al. A prospective comparison of ^{18}F-prostate-specific membrane antigen-1007 positron emission tomography computed

tomography, whole-body 1.5 T magnetic resonance imaging with diffusion-weighted imaging, and single-photon emission computed tomography/computed tomography with traditional imaging in primary distant metastasis staging of prostate cancer (PROSTAGE). *Eur Urol Oncol.* 2021;4:635–644.
10. Hofman MS, Lawrentschuk N, Francis RJ, et al. Prostate-specific membrane antigen PET-CT in patients with high-risk prostate cancer before curative-intent surgery or radiotherapy (proPSMA): a prospective, randomised, multicentre study. *Lancet.* 2020;395:1208–1216.
11. Sonni I, Eiber M, Fendler WP, et al. Impact of ^{68}Ga-PSMA-11 PET/CT on staging and management of prostate cancer patients in various clinical settings: a prospective single-center study. *J Nucl Med.* 2020;61:1153–1160.
12. Fendler WP, Calais J, Eiber M, et al. Assessment of ^{68}Ga-PSMA-11 PET accuracy in localizing recurrent prostate cancer: a prospective single-arm clinical trial. *JAMA Oncol.* 2019;5:856–863.
13. Afshar-Oromieh A, Malcher A, Eder M, et al. PET imaging with a [^{68}Ga]gallium-labelled PSMA ligand for the diagnosis of prostate cancer: biodistribution in humans and first evaluation of tumour lesions. *Eur J Nucl Med Mol Imaging.* 2013; 40:486–495.
14. Robu S, Schmidt A, Eiber M, et al. Synthesis and preclinical evaluation of novel ^{18}F-labeled Glu-urea-Glu-based PSMA inhibitors for prostate cancer imaging: a comparison with ^{18}F-DCFPyl and ^{18}F-PSMA-1007. *EJNMMI Res.* 2018;8:30.
15. Herrmann K, Bluemel C, Weineisen M, et al. Biodistribution and radiation dosimetry for a probe targeting prostate-specific membrane antigen for imaging and therapy. *J Nucl Med.* 2015;56:855–861.
16. Maurer T, Gschwend JE, Eiber M. Prostate-specific membrane antigen-guided salvage lymph node dissection in recurrent prostate cancer. *Curr Opin Urol.* 2018;28:191–196.
17. Robu S, Schottelius M, Eiber M, et al. Preclinical evaluation and first patient application of ^{99m}Tc-PSMA-I&S for SPECT imaging and radioguided surgery in prostate cancer. *J Nucl Med.* 2017;58:235–242.
18. Brunello S, Salvarese N, Carpanese D, Gobbi C, Melendez-Alafort L, Bolzati C. A review on the current state and future perspectives of [^{99m}Tc]Tc-housed PSMA-i in prostate cancer. *Molecules.* 2022;27:2617.
19. Werner P, Neumann C, Eiber M, Wester HJ, Schottelius M. [^{99cm}Tc]Tc-PSMA-I&S-SPECT/CT: experience in prostate cancer imaging in an outpatient center. *EJNMMI Res.* 2020;10:45.
20. Rajasekaran SA, Anilkumar G, Oshima E, et al. A novel cytoplasmic tail MXXXL motif mediates the internalization of prostate-specific membrane antigen. *Mol Biol Cell.* 2003;14:4835–4845.
21. Maurer T, Robu S, Schottelius M, et al. ^{99m}Technetium-based prostate-specific membrane antigen-radioguided surgery in recurrent prostate cancer. *Eur Urol.* 2019;75:659–666.
22. Rosset A, Spadola L, Ratib O. OsiriX: an open-source software for navigating in multidimensional DICOM images. *J Digit Imaging.* 2004;17:205–216.
23. Rasch D, Kubinger KD, Moder K. The two-sample t test: pre-testing its assumptions does not pay off. *Stat Pap (Berl).* 2011;52:219–231.
24. Ruxton GD. The unequal variance t-test is an underused alternative to Student's t-test and the Mann-Whitney U test. *Behav Ecol.* 2006;17:688–690.
25. Q04609 FOLH1_HUMAN. UniProt website. https://www.uniprot.org/uniprot/Q04609. Accessed May 2, 2023.
26. Afshar-Oromieh A, Hetzheim H, Kübler W, et al. Radiation dosimetry of ^{68}Ga-PSMA-11 (HBED-CC) and preliminary evaluation of optimal imaging timing. *Eur J Nucl Med Mol Imaging.* 2016;43:1611–1620.
27. Fendler WP, Eiber M, Beheshti M, et al. ^{68}Ga-PSMA PET/CT: joint EANM and SNMMI procedure guideline for prostate cancer imaging—version 1.0. *Eur J Nucl Med Mol Imaging.* 2017;44:1014–1024.
28. Rahbar K, Afshar-Oromieh A, Bögemann M, et al. ^{18}F-PSMA-1007 PET/CT at 60 and 120 minutes in patients with prostate cancer: biodistribution, tumour detection and activity kinetics. *Eur J Nucl Med Mol Imaging.* 2018;45:1329–1334.
29. Albalooshi B, Al Sharhan M, Bagheri F, et al. Direct comparison of ^{99m}Tc-PSMA SPECT/CT and ^{68}Ga-PSMA PET/CT in patients with prostate cancer. *Asia Ocean J Nucl Med Biol.* 2020;8:1–7.
30. Fallahi B, Khademi N, Karamzade-Ziarati N, et al. ^{99m}Tc-PSMA SPECT/CT versus ^{68}Ga-PSMA PET/CT in the evaluation of metastatic prostate cancer. *Clin Nucl Med.* 2021;46:e68–e74.
31. Rauscher I, Düwel C, Wirtz M, et al. Value of ^{111}In-prostate-specific membrane antigen (PSMA)-radioguided surgery for salvage lymphadenectomy in recurrent prostate cancer: correlation with histopathology and clinical follow-up. *BJU Int.* 2017;120:40–47.
32. Urbán S, Meyer C, Dahlbom M, et al. Radiation dosimetry of ^{99m}Tc-PSMA I&S: a single-center prospective study. *J Nucl Med.* 2021;62:1075–1081.